Metrol. Meas. Syst., Vol. 30 (2023) No. 1, pp. 17–30
DOI: 10.24425/mms.2023.144403

PAN POLSKA AKADEMIA NAUK

METROLOGY AND MEASUREMENT SYSTEMS

Index 330930, ISSN 0860-8229
www.metrology.wat.edu.pl

M&MS

STANDARD DEVIATION IN THE SIMULATION OF STATISTICAL MEASUREMENTS

Krzysztof Przystupa[1)], Zenoviy Kolodiy[2)], Svyatoslav Yatsyshyn[2)], Jacek Majewski[3)], Yuriy Khoma[2)], Iryna Petrovska[2)], Serhiy Lasarenko[2)], Taras Hut[2)]

1) Department Automation, Lublin University of Technology, ul. Nadbystrzycka 36, 20-618 Lublin, Poland (✉ *k.przystupa@pollub.pl*)
2) Lviv Polytechnic National University, Institute of Computer Technologies, Automatics and Metrology, S. Bandera Str. 28a, 79013, Lviv, Ukraine (*zenovii.o.kolodii@lpnu.ua, sviatoslav.p.yatsyshyn@lpnu.ua, yurii.v.khoma@lpnu.ua, iryna.r.petrovska@lpnu.ua, serhii.l.lazarenko@lpnu.ua, taras.p.hut@lpnu.ua*)
3) Department of Automation and Metrology, Lublin University of Technology, ul. Nadbystrzycka 38D, 20-618 Lublin, Poland (*j.majewski@pollub.pl*)

Abstract

Is this article simulation of statistical measurements is performed on the basis of which the analysis of the standard deviation of the obtained results is carried out. It is shown that the standard deviation is minimum and independent from measurement duration while an object is in the state of equilibrium. For objects in a stationary non-equilibrium state the standard deviation depends on the duration measurements and the parameters of the state. The influence of these factors on the standard deviation is assessed with equation which includes the relaxation time. The value of the relaxation time is determined by approximating the energy spectrum of the studied signals. The analysis of energy spectra showed that the spectrum of white noise is inherent in objects in equilibrium; the flicker component of the spectrum occurs when the state of the object deviates from equilibrium.

Keywords: standard deviation, measurement, relaxation time, energy spectrum.

1. Introduction

In statistical measurements of the physical quantity $X(t)$, the measurement results are obtained in the form of time series $x_1(t), x_2(t), \ldots, x_k(t)$ [1, 2], looking graphically as the deviations of the measured value from the mean, and carry some information [3–5]. While processing such results, first of all the mean value $\overline{X}$ and its variance $D_{\overline{X}}$ are determined. If the obtained results are independent, then according to the central limit theorem, the variance should decrease with the number of measurements N as $D_{\overline{X}} = \dfrac{\sigma_x^2}{N}$ [1, 6]. Here σ_x is the standard deviation (SD) of the single measurement. That is, for the independent multiple measurements, the random error

Article history: received July 3, 2022; revised December 3, 2022; accepted December 6, 2022; available online February 11, 2023.

characterized by the variance $D_{\overline{X}}$ or SD $\sigma_{\overline{x}} = \sqrt{D}_{\overline{X}} = \dfrac{\sigma_x}{\sqrt{N}}$ can be reduced to an arbitrarily small value by increasing the number of measurements N.

However, an increase in the number of N requires the prolongation of measurements T_m, and the condition of independence of the measurement results does not unambiguously consider the drift of the measured value over time. While measuring, the physical quantities alter permanently. Thus, the statistical stability of the obtained means is broken. In addition, in [7] has been found that the variance of the mean value first decreases and later stabilizes with the number of measurements or their duration enlargement.

This article aims to simulate statistical measurements and analyze the dependence of the standard deviation on their duration and also experimental verification of theoretical statements.

2. Simulation of statistic measurements

Statistical measurements of "potential difference" or "voltage" were simulated by the difference in the number of moving elementary balls Δn, which within Δt have touched the left and right rectangle sides. While computing, it was deployed the inner vertical partitions that change the structure of the object under study (Fig. 1).

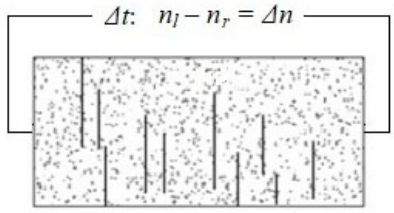

Fig. 1. View of the computer model of the "potential difference" measurement.

Before starting the simulation, the following is set: rectangle size, number of balls, number and coordinates of partitions, partition lengths, parameters of velocity, parameters of balls normal distribution (mean value $\overline{\vartheta}$ and standard deviation $\Delta\vartheta$), measurement duration T_{meas}, and sampling interval Δt.

In the process of chaotic movement of balls over the considered area, it happens that, due to their elasticity, they bounce from the sides of the rectangle and partitions. This model is similar to the model [8] of the snooker applied to generate random noise of arbitrary statistical properties.

First, simulations were performed for a model simulating an equilibrium system – a rectangle without partitions, in which the probability of finding an elementary ball in any place of the rectangle is the same. Later, we consider a model that simulates a stationary non-equilibrium system – a rectangle with partitions where the probability of finding an elementary sphere in any place of the rectangle is not the same due to the presence of partitions. It takes some time τ_0 to restore equal probability. Figure 2 shows the appearance of the models of equilibrium and stationary non-equilibrium systems, as well as corresponding histograms of measurement results.

When modeling statistical measurements, the variable parameters of the models were only the number, length, and location of partitions. Other simulation parameters *i.e.*, the size of the rectangle, the number of elementary balls, mean velocity and its standard deviation, duration

Metrol. Meas. Syst., Vol. 30 (2023), No. 1, pp. 17–30
DOI: 10.24425/mms.2023.144403

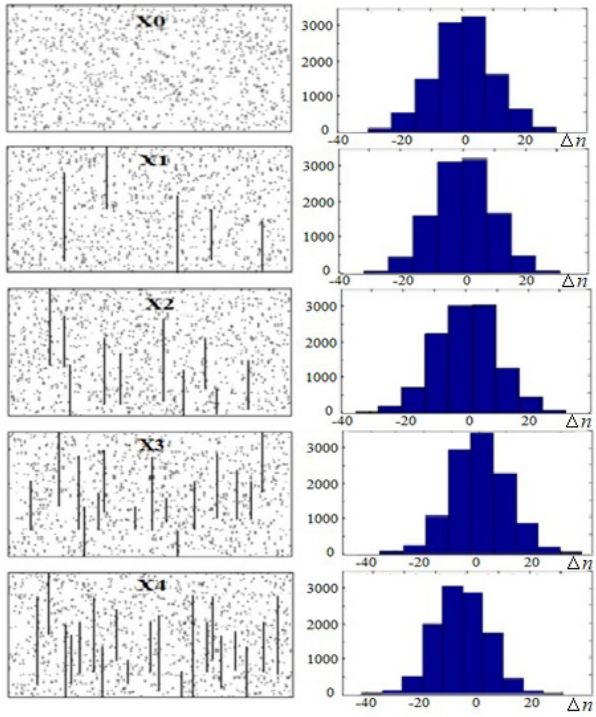

Fig. 2. Models of equilibrium (X0) and stationary non-equilibrium systems (X1–X4) and corresponding histograms of measurement results.

of the simulation, and number of results – were permanent for all models. The time series of simulated results of statistical measurements are as shown in Fig. 3, where m is the number of samples.

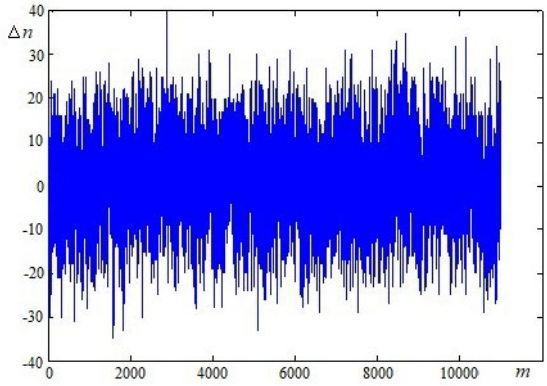

Fig. 3. Time series of simulated results of statistical measurements.

Before starting the model, the number, length and location of the partitions are fixed and remain unchanged until the end of the simulation. Therefore, we obtain time series of results of

measuring "potential difference" or "voltage" with time-invariant parameters of the object. If the measurement results are independent, then, according to the central limit theorem, the law of distribution of such results approaches the normal law. Figure 2 shows that the histograms for models X0 and X1 are similar to the normal distribution law. That is, for balanced (X0) and weakly unbalanced objects (X1) independence of measurement results and their normal distribution law are characteristic. Some difference between the histograms for models of unbalanced objects X2–X4 from the normal distribution law may indicate a certain interdependence of measurement results obtained for unbalanced objects.

From the total number of 11000 measurement results 50 groups were selected ($N = 50$ groups of measurements have been performed). It should be explained here that within each group $k = 100$ consecutive measurements at time intervals Δt were performed. The considered groups were placed randomly along the t axis in Fig. 4.

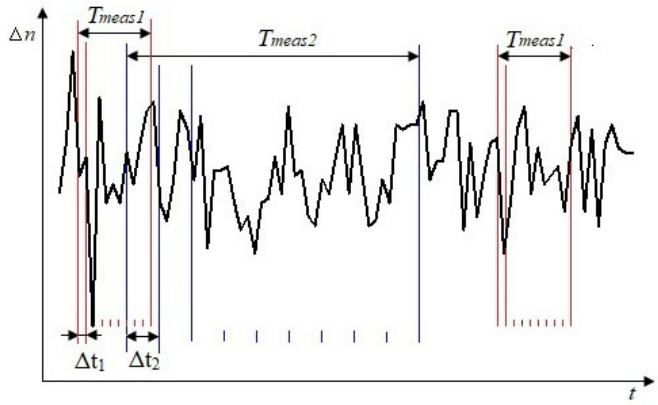

Fig. 4. Placement of sample groups.

While processing the results of measurements for each model based on the sampling of 50 groups, the means $\overline{X}$ and SD $\sigma_{\overline{x}}$ of means at different Δt (at different T_m) were determined (Table 1):

Table 1. Dependence of the standard deviation $\sigma_{\overline{x}}$ of the mean value of 50 sample groups on the measurement duration T_m.

Δt [s]	$T_m = k\Delta t$ [s]	X0: $\overline{X0} = 0.036$; $\sigma_x = 9.800$		X1: $\overline{X1} = -0.286$; $\sigma_x = 9.930$		X2: $\overline{X2} = 0.967$; $\sigma_x = 9.716$		X3: $\overline{X3} = 0.148$; $\sigma_x = 9.982$		X4: $\overline{X4} = -1.059$; $\sigma_x = 10.649$	
		$\overline{X}$	$\sigma_{\overline{x}}$	$\overline{X}$	$\sigma_{\overline{x}}$	$\overline{X}$	$\sigma_{\overline{x}}$	$\overline{X}$	$\sigma_{\overline{x}}$	$\overline{X}$	$\sigma_{\overline{x}}$
0.01	1	0.036	0.922	–0.254	1.917	1.031	2.122	0.286	3.333	–0.715	3.736
0.05	5	0.136	0.860	–0.920	1.162	0.917	1.295	0.476	1.748	0.850	1.471
0.1	10	0.112	0.920	–0.771	1.121	0.565	1.568	0.415	1.438	0.105	1.969
0.5	50	0.060	0.793	–0.668	0.854	0.902	0.798	0.448	1.103	0.608	1.274
1	100	0.152	0.869	–0.417	0.944	1.043	0.803	0.184	0.806	-0.794	1.188

The upper row of Table 1 shows the means and their SDs of the whole set of measurement results (11000 results at $\Delta t = 0.01$ s, $T_m = 110$ s) for each model. The dependence of $\sigma_{\overline{x}}$ on T_m is shown in Fig. 5. Analyzing these results, we can conclude that:

Metrol. Meas. Syst., Vol. 30 (2023), No. 1, pp. 17–30
DOI: 10.24425/mms.2023.144403

1. For the model of the equilibrium system X0, the value of $\sigma_{\overline{x}} \approx 0.9$ almost does not depend on T_m.
2. For models of non-equilibrium systems X1–X4 the value of $\sigma_{\overline{x}}$ decreases with T_m, and for X4 the value of $\sigma_{\overline{x}}$ at $T_m = 1$ s is the largest.
3. At $T_m = 100$ s, the value of $\sigma_{\overline{x}}$ is approximately the same for the models of equilibrium X0 and non-equilibrium X1–X4 systems.

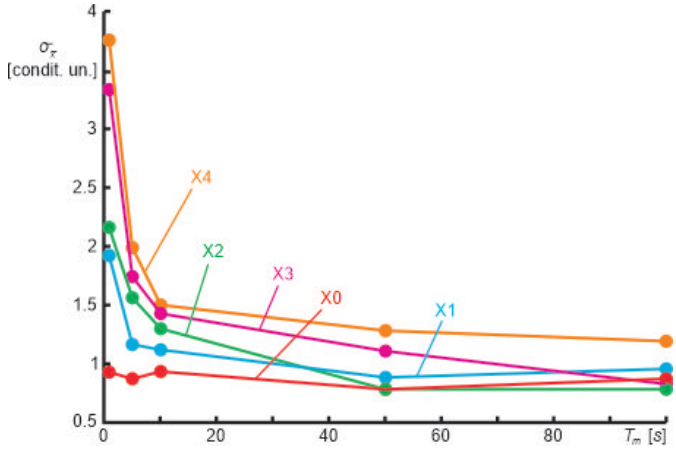

Fig. 5. Dependence of the standard deviation $\sigma_{\overline{x}}$ of the mean of models X0–X4 on the measurement duration T_m. (Data are received from the above Table 1)

Figure 5 testifies that the more partitions contains the model, the more evident becomes the dependence of $\sigma_{\overline{x}}$ on T_m.

Table 2 and Fig. 6 show the dependences of SD $\sigma_{\overline{x}}$ on the number of measurements k at the same duration of T_m (for instance, for models X0, X3, and X4).

Table 2. Dependences of SD $\sigma_{\overline{x}}$ on the number of measurements k at the same duration of T_m.

Δt [s]	k	T_m [s]	N	X0	X3	X4
				$\sigma_{\overline{x}}$		
0.01	100	1	50	0.922	3.333	3.736
0.05	20	1	50	1.854	3.361	3.679
0.1	10	1	50	3.202	4.434	3.442
0.05	100	5	50	0.860	1.748	1.471
0.1	50	5	50	1.328	2.359	2.441
0.5	10	5	50	2.989	3.211	2.778
0.1	100	10	50	0.920	1.434	1.945
0.5	20	10	50	2.440	2.427	1.954
1.0	10	10	50	3.036	3.188	3.080
0.5	100	50	50	0.793	1.103	1.274
1	50	50	50	1.105	1.474	1.409

Note: here N is the number of measurements/groups, which determines the means and their SDs.

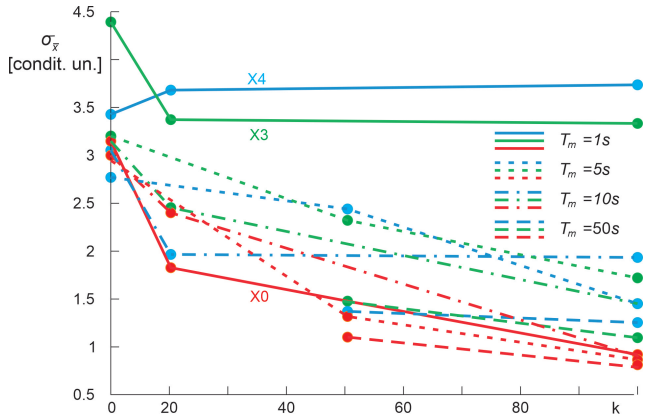

Fig. 6. Dependence of the standard deviation $\sigma_{\overline{x}}$ on the number of results k at the same measurement duration T_m for a particular group.

It can be seen (Table 2 and Fig. 6) that only for model X0 the dependence of σ on the number of measurements k is close to that previously estimated by the formula: $\sigma = \sqrt{\frac{1}{k}\sum_{i=1}^{k}(x_i - \overline{x})^2}$, regardless of the duration T_m. For models X3 and X4, the dependences of σ on the number of measurements at small values of T_m are not similar to model X0 [9].

Analysis of the data (Table 1 and Table 2, Fig. 5 and Fig. 6) gives grounds to check the well-known expressions for SD applied for assessing results of measurements for the objects in a state of equilibrium [10, 11]. To evaluate similar results for objects in a stationary non-equilibrium state, it seems necessary to take into account the error $\Delta\sigma_{\overline{x}}$ caused by the measurement duration. The value of the latter decreases (Fig. 5) with T_m as [12]:

$$\Delta\sigma_{\overline{x}} \approx \frac{C}{\sqrt{F_e T_m}} \tag{1}$$

where F_e is the equivalent band of the signal stochastic spectrum (the time series in Fig. 3 is an example of such signal); C is a constant, dependent on the shape of the spectrum.

The additional error depends on the state of the object under study [13–15] (Fig. 5). If we estimate the non-equilibrium of the model by the number of partitions, then the farther from the equilibrium the model (X4) is, the greater the additional error. Depending on the state of the object, this error could be estimated applying a parameter for non-equilibrium. Such parameter is considered to be the relaxation time τ. It goes to infinity for the equilibrium system. So, for the equilibrium system the additional error $\Delta\sigma_{\overline{x}}$ with its inversely proportional to τ go to zero.

Since the SD of the measured parameters of the equilibrium object is independent of measurement duration (Table 1, Fig. 5), it becomes minimal for this method of measurement (with the given number of measurements and obtained results). Then the general expression for SD of the parameters of the stationary non-equilibrium object must contain 2 components. One is the minimal value of SD inherent in the equilibrium object; the other component is the SD, dependent on measurement duration (1) and the state of the object:

$$\sigma_H = \sigma_0 \left(1 + \frac{C}{\sqrt{(T_m + \tau)\Delta f}}\right), \tag{2}$$

Metrol. Meas. Syst., Vol. 30 (2023), No. 1, pp. 17–30
DOI: 10.24425/mms.2023.144403

where $\sigma_0 = \frac{\sigma}{\sqrt{N}}$, N is the number of measurement groups; Δf is the bandwidth of the studied process. From (2), the additional error, which depends on the object state with $0 < \tau \ll \infty$, becomes noticeable at $T_m \leq \tau$, *i.e.*, at small values of T_m (Fig. 4). For $T_m > \tau$, $\sigma_H \to \sigma_0$.

Formula (2) makes it possible to correctly estimate the measurement error of parameters of real objects (non-equilibrium objects). With known T_m, Δf and determined τ, the measurement error can be calculated *a priori*. Analysis of Formula (2) shows that in order to reduce σ_H with a short duration of T_m measurements, it is necessary to increase the equilibrium of the research object itself ($\tau \gg 0$).

The simulation results collected in Table 1 and depicted in Fig. 5 were compared with the results of analysis of measurements of the means and SDs for stochastic signals of *electroencephalogram* (EEG) measurements of 6 patients. The signals EEG-2, EEG-2-1, EEG-2-2 were recorded from the problem area of the brain (tumor) and the signals EEG-3, EEG-3-1, EEG-3- 2 were recorded from a healthy area of the brain. The duration of the recording of each EEG was 23 s at the sampling frequency of 178 Hz. The number of digitized EEG results was 4094 (Fig. 7).

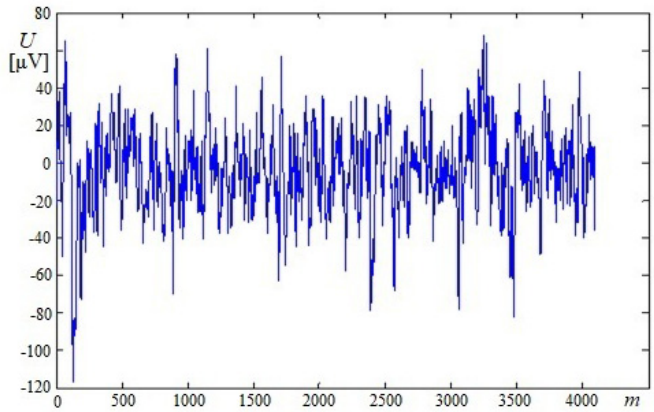

Fig. 7. Time series of electroencephalogram measurement results.

Similarly to computer models, while processing the results of EEG measurements of each patient based on the means of 50 groups of 100 results in each group were calculated by the mean $\overline{U}$ and SDs $\sigma_{\overline{U}}$ of means at different T_m (Table 3, Table 4).

Table 3. Dependence of the standard deviations $\sigma_{\overline{U}}$ of the mean value of electroencephalograms recorded from the problem area of the brain on the measurement duration T_m.

Δt [s]	T_m [s]	EEG-2		EEG-2-1		EEG-2-2	
		$\overline{U}$ [μV]	$\sigma_{\overline{U}}$ [μV]	$\overline{U}$ [μV]	$\sigma_{\overline{U}}$ [μV]	$\overline{U}$ [μV]	$\sigma_{\overline{U}}$ [μV]
0.0056	0.56	–31.77	13.64	22.92	20.41	12.68	17.52
0.028	2.8	–32.32	3.63	25.15	4.41	11.79	9.90
0.056	5.6	–32.14	2.33	24.00	3.86	10.75	4.71
0.112	11.2	–32.17	1.793	24.34	3.68	11.80	2.14
0.225	22.5	–31.07	4.623	21.95	3.89	13.53	1.58

Table 4. The dependence of the standard deviations $\sigma_{\overline{U}}$ of the mean value of electroencephalograms recorded from a healthy area of the brain on the measurement duration T_m.

Δt [s]	T_m [s]	EEG-3		EEG-3-1		EEG-3-2	
		$\overline{U}$ [μV]	$\sigma_{\overline{U}}$ [μV]	$\overline{U}$ [μV]	$\sigma_{\overline{U}}$ [μV]	$\overline{U}$ [μV]	$\sigma_{\overline{U}}$ [μV]
0.0056	0.56	–4.21	10.44	1.51	27.51	–40.69	15.83
0.028	2.8	–4.26	2.34	4.33	11.34	–36.03	7.77
0.056	5.6	–3.46	2.22	3.77	7.19	–39.91	4.60
0.112	11.2	–4.30	1.49	3.43	2.78	–38.19	3.87
0.225	22.5	–4.25	1.72	0.39	2.73	–38.95	1.29

The maximum value of $\Delta t_{\max} = 0.225$ s in each group is limited by the condition of the same number of results for both model and EEG that is 50 groups of 100 measurement results with a total EEG duration of 23 s. The value of $\Delta t_{\min} = \Delta t_\delta = 1/f_\delta = 0.0056$ s. The graphs of the dependence of SD $\sigma_{\overline{U}}$ of the EEG means on the measurement duration T_m are indicated in Fig. 8.

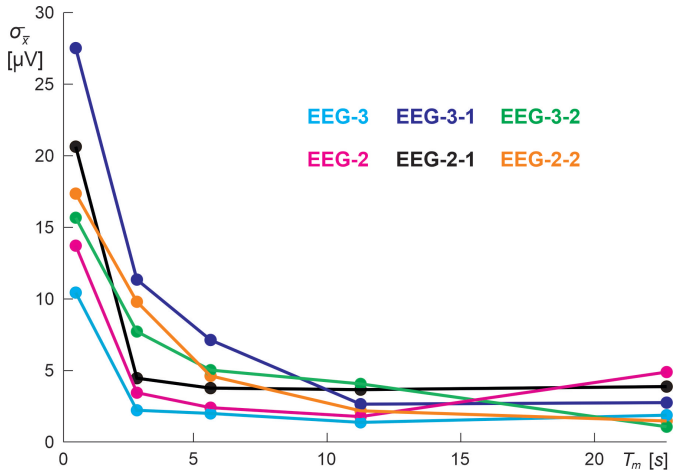

Fig. 8. Dependence of the standard deviation $\sigma_{\overline{x}}$ of the EEG mean value on the measurement duration T_m.

The comparison of Fig. 5 and Fig. 8 shows that the dependence SD on the duration of EEG measurement is quite similar to the model of the stationary non-equilibrium system, *i.e.*, decreases with T_m. Such dependence is specific for each EEG. The individuality of the $\sigma_{\overline{x}}(T_m)$ for the studied and simulated (X1–X4) dependences is especially noticeable at initial values of T_m. Based on the above-mentioned obtained results for simulated and studied dependences (Fig. 5, Fig. 8), we propose to determine (according to Formula (2)) the random error caused by the finite measurement duration. This permits us to consider the peculiarity of each studied process through the relaxation time.

The latter being within interval $0 < \tau \ll \infty$ is characteristic of the non-equilibrium system. The criterion of equilibrity corresponds to the invariance of energy spectrum of the studied signals in the whole bandwidth, starting from $f \to 0$. The definition of the energy spectrum may be recommended based on [7], in which it "is established that the violation of the statistical stability of the mean is associated with the peculiarities of the spectrum of the considered process". The

Metrol. Meas. Syst., Vol. 30 (2023), No. 1, pp. 17–30
DOI: 10.24425/mms.2023.144403

energy spectrum of $W(f)$ signals of models X0–X4 was determined in two ways. One is the modeling of the signal energy spectra. The other consists of computing the energy spectra with help of correlation functions. The block scheme of the measurement model is shown in Fig. 9.

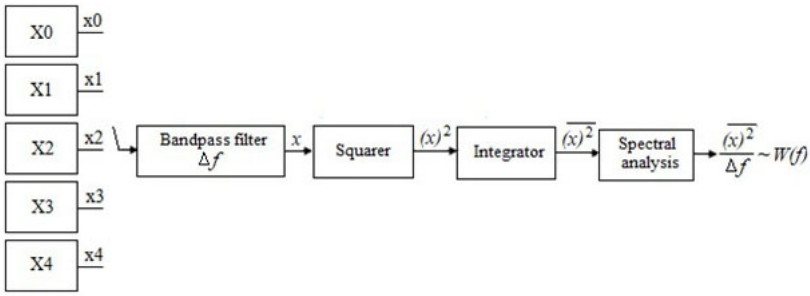

Fig. 9. Block-scheme of the measurement model of the signals' energy spectra.

The bandpass filter is modeled as a digital non-recursive filter with the quality factor of 50.0 within the measured bandwidth and attenuation ~60 dB of the signal at the edges. The squarer, integrator and spectrum analyzer are implemented in the software. Table 5 presents the results of energy spectra of models X0–X4 (Fig. 10).

Table 5. Energy spectra of signals of models X0–X4.

f_0 [Hz]	Δf [Hz]	X0	X1	X2	X3	X4
		$W(f)$ [conditional units]				
1.01	0.02	1.88	5.47	7.04	10.24	22.89
2.02	0.04	1.97	4.23	5.19	6.68	6.18
5.05	0.1	1.92	3.97	4.12	3.42	4.66
+10.1	0.2	1.93	2.60	2.84	2.62	2.91
25.25	0.5	2.06	2.38	2.16	1.62	1.97
40.4	0.8	1.90	2.09	1.81	1.77	1.65

f_0 is average frequency; Δf is the bandwidth of the bandpass filter.

Figure 10 shows the graphs of signal energy spectra of models X0–X4, measured with a digital filter and determined by correlation functions.

Analyzing the energy spectra (Fig. 10), we can note the following features:

1. Energy spectra $W(f)$, determined with help of the digital filter, are similar to the spectra determined by autocorrelation functions. This indicates the acceptability of both methods as well as correct consideration of energy spectra.
2. The energy spectrum of model X0 is permanent within the bandwidth of 1.0–40.0 Hz (which is similar to the white noise spectrum); so, model X0 represents an equilibrium object.
3. The energy spectra of models X1–X4 increase with the falling frequency which is highly noticeable for model X4. Enhancement of the spectrum with decreasing frequency is characteristic of flicker noise [16–19] (see Fig. 10, dependence $1/f$). Fig. 10 also shows

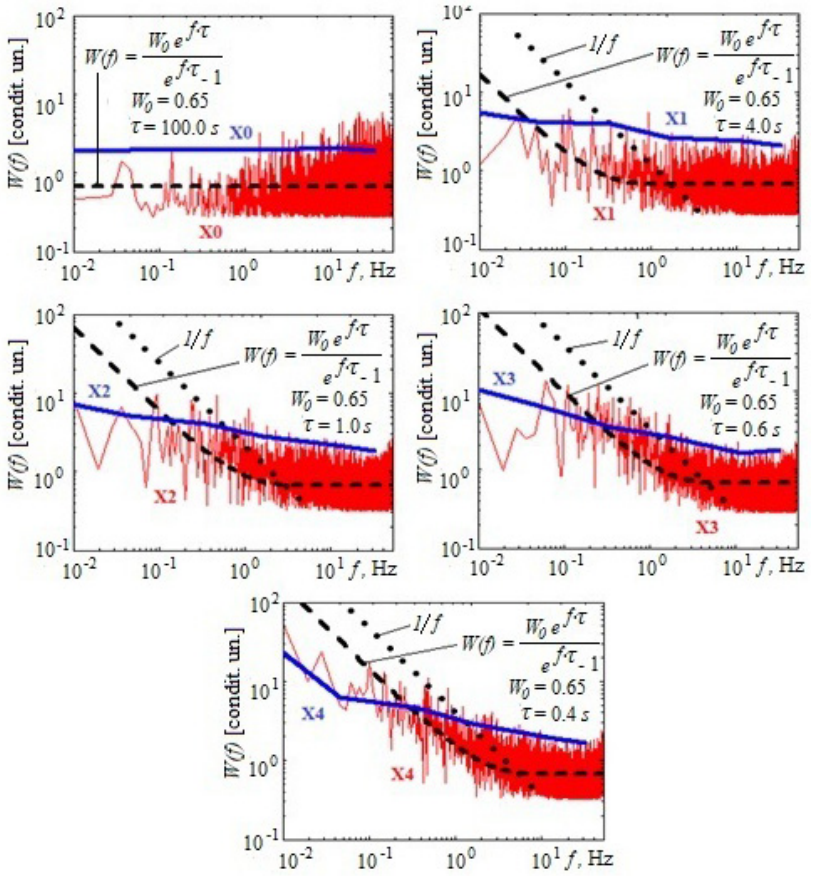

Fig. 10. Signals' energy spectra of models X0–X4, measured using a digital filter (blue) and determined by their correlation functions (red).

the approximation of the obtained energy spectra by the formula [20]:

$$W(f) = \frac{W_0 e^{f\tau}}{e^{f\tau} - 1}, \tag{3}$$

which, in our opinion, corresponds to the given spectra of models X0–X4. The values of W_0 (minimum of the spectrum) and relaxation time τ were determined according to [21].

4. The inequality of energy spectra of models X1–X4 in the studied frequency band gives grounds to classify these models as non-equilibrium objects.
5. The value of τ in the approximation dependence (3) decreases with the partition number of models X1–X4.

For verification of the spectra behavior as in Fig. 10, the time series x0, x1, x2, x3, x4 (Fig. 7) were converted into soundtracks with their subsequent listening. At the same time, the soundtracks x0 and x4 mutually differ the most: for x0 the sound is uniform, for x4 the low-frequency components are of greater intensity.

The methods above were applied to determine the energy spectra for EEGs: 2, 2–1, 2–2, 3, 3–1, 3–2 (Fig. 11). Spectra amplify with decreasing frequency, similar to the computer models

Metrol. Meas. Syst., Vol. 30 (2023), No. 1, pp. 17–30
DOI: 10.24425/mms.2023.144403

X1–X4 [22,23]. For comparison, Fig. 11 shows the flicker-noise spectrum of the A/f type (factor A was determined by selection) and the approximation of the spectra by Equation (3). Finally, we can conclude that EEGs of Fig. 11, as well as models X1–X4, are described by the signals of non-equilibrium systems.

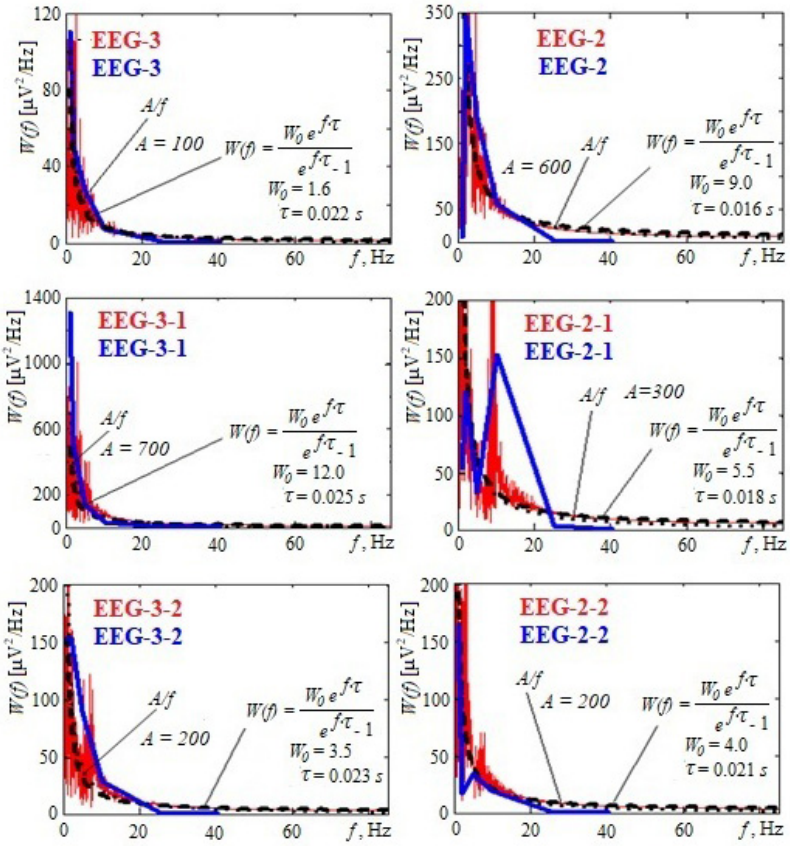

Fig. 11. Energy spectra of electroencephalograms.

The determined values of τ (Fig. 10, Fig. 11) were substituted in (2) for estimating the error σ_H of measuring the means of the signals X0–X4 and EEGs. Factor C of (2) was selected experimentally, considering the shape of the spectra of Fig. 10, Fig. 11. Table 6 shows the values of SD determined by (2) for the signals of models X1–X4, where σ_0 is defined as the SD mean for model X0 (Table 1). The bandwidth is counted as $\Delta f = 1/2\Delta t_{\min} = 1/2 \cdot 0.01 = 50$ Hz.

In Table 6, the parentheses have specified the deviations of σ_H from the values of $\sigma_{\overline{x}}$ (Table 1). Significant deviations (46%, 54%) are most likely related to the inexactness of the determination of σ_0 and C. Table 7 shows the σ_H values determined according to (2) for EEG-3; EEG 3-1, since the spectra of these signals are marked by fewer peaks compared to the spectra of the other EEGs (Fig. 11). This makes it possible to determine τmore accurately. The deviations of σ_H from the values in Table 4 may be caused by the approximation of σ_0 and C.

The results of the current work are valuable for estimating the errors of the object parameters, especially at small measurement duration.

Table 6. SD means of the results for models X1–X4 considering the relaxation time τ.

T_m [s]	Δf [Hz]	X1: τ = 4.0 [s] C = 10, σ_0 = 0.9	X2: τ = 1.0 [s] C = 15, σ_0 = 0.9	X3: τ = 0.6 [s] C = 20, σ_0 = 0.9	X4: τ = 0.4 [s] C = 25, σ_0 = 0.9
		σ_H			
1	50	1.47 (-24%)	2.25 (6%)	2.91 (–13%)	3.59 (–4%)
5	50	1.32 (14%)	1.68 (30%)	1.98 (13%)	2.27 (54%)
10	50	1.24 (10%)	1.48 (–6%)	1.68 (17%)	1.89 (–4%)
50	50	1.07 (25%)	1.17 (46%)	1.26 (14%)	1.35 (6%)
100	50	1.02 (9%)	1.09 (36%)	1.15 (43%)	1.22 (3%)

Table 7. SD means of the EEG measurements considering the relaxation time τ.

T_m [s]	Δf [Hz]	EEG-3: τ = 0.022 [s], C = 30, σ_0 = 1.72 [μV]	EEG-3-1: τ = 0.025 [s], C = 55, σ_0 = 2.73 [μV]
		σ_H [μV]	
0.56	89	8.90 (–15%)	23.54 (–15%)
2.8	89	4.98 (113%)	12.20 (8%)
5.6	89	4.03 (81%)	9.44 (31%)
11.2	89	3.36 (125%)	7.48 (169%)
22.5	89	2.87 (67%)	6.08 (122%)

3. Conclusions

The *standard deviation* (SD) of the means of the objects' parameters in the state of equilibrium does not depend on the measurement duration and, with the selected number of measurement series and results, it becomes minimal.

For non-equilibrium objects, SD depends on the measurement duration: as the measurement duration increases, SD decreases to the level of the SD for objects in the equilibrium state. SD depends on the degree of the object under study deviation from the equilibrium: the farther from it the object is, the greater the standard deviation, especially at low measurement durations. An expression for the standard deviation of the means of the parameters of objects in a stationary non-equilibrium state contains two components: the first one applied to the object in an equilibrium state, is minimal; the second one is inversely proportional to the measurement duration and relaxation time as well as the bandwidth of the signal spectrum.

From the analysis of simulation results it follows that fluctuations in the parameters of the object at equilibrium acquire the form of white noise, and a rise of the energy spectrum at $f \to 0$ *i.e.*, the flicker component of the spectrum occurs for an object in a non-equilibrium state.

References

[1] DeCoursey, W. (2003). *Statistics and Probability for Engineering Applications*. Elsevier.

[2] Box, G. E. P., Jenkins, G. M., & Reinsel, G. C. (1994). *Time Series Analysis: Forecasting and Control* (3rd ed.). Prentice-Hall.

Metrol. Meas. Syst., Vol. 30 (2023), No. 1, pp. 17–30
DOI: 10.24425/mms.2023.144403

[3] Jun, S., & Kochan, O. (2015). Common mode noise rejection in measuring channels. *Instruments and Experimental Techniques*, *58*(1), 86–89. https://doi.org/10.1134/S0020441215010091

[4] Jebb, A. T., Tay, L., Wang, W., & Huang, Q. (2015). Time series analysis for psychological research: examining and forecasting change. *Frontiers in Psychology*, *6*, 727. https://doi.org/10.3389/fpsyg.2015.00727

[5] Xu, H., Przystupa, K., Fang, C., Marciniak, A., Kochan, O., & Beshley, M. (2020). A combination strategy of feature selection based on an integrated optimization algorithm and weighted k-nearest neighbor to improve the performance of network intrusion detection. *Electronics*, *9*(8), 1206. https://doi.org/10.3390/electronics9081206

[6] Kirkup, L., & Frenkel, R. B. (2006). *An introduction to uncertainty in measurement: using the GUM* (Guide to the Expression of Uncertainty in Measurement). Cambridge University Press.

[7] Gorban', I. I. I. (2018). Estimation of statistically unpredictable changes in physical quantities over large observation intervals. *Technical Physics*, *63*, 1722–1729. https://doi.org/10.1134/S106378421812006X

[8] Chichigina, O., & Valenty, D. (2021). Strongly super-Poisson statistics replaced by a wide-pulse Poisson process: the billiard random generator. *Chaos, Solitons and Fractals*, *153*(1), 111451. https://doi.org/10.1016/j.chaos.2021.111451

[9] Kolodiy, Z., Stadnyk, B., & Yatsyshyn, S. (2013). Development of Noise Measurements. Part 2. Random Error. *Sensors & Transducers*, *151*(4), 107-112.

[10] Curran-Everett, D. (2008). Explorations in statistics: standard deviations and standard errors. *Advances in Physiology Education*, *32*, 203–208. https://doi.org/10.1152/advan.90123.2008

[11] Jun, S., Przystupa, K., Beshley, M., Kochan, O., Beshley, H., Klymash, M., Wang, J., & Pieniak, D. (2020). A cost-efficient software based router and traffic generator for simulation and testing of IP network. *Electronics*, *9*(1), 40. https://doi.org/10.3390/electronics9010040

[12] Makarov, S. V., Medvedev, S. Y., & Yakimov, A. V. (2000). Correlation between the Intensities of Spectral Components of 1/f Noise. *Radiophysics and Quantum Electronics*, *43*(11), 916–922. https://doi.org/10.1023/A:1010361619798

[13] Jun, S., Kochan, O., & Kochan, R. (2016). Thermocouples with built-in self-testing. *International Journal of Thermophysics*, *37*(4), 1–9. https://doi.org/10.1007/s10765-016-2044-2

[14] Mohajan, H. K. (2017). Two Criteria for Good Measurements in Research: Validity and Reliability. *Annals of Spiru Haret University*, *17*(4), 59–82.

[15] Jun, S., Kochan, O., Kochan, V., & Wang, C. (2016). Development and investigation of the method for compensating thermoelectric inhomogeneity error. *International Journal of Thermophysics*, *37*(1), 1–14. https://doi.org/10.1007/s10765-015-2025-x

[16] Kwon, J., Delker, C. J., Harris, C. T., Das, S. R., & Janes, D. B. (2020). Experimental and modeling study of 1/f noise in multilayer MoS_2 and $MoSe_2$ field-effect transistors. *Journal of Applied Physics*, *128*, 094501. https://doi.org/10.1063/5.0014759

[17] Deng, W., & Fossum, E. R. (2019). 1/f Noise Modelling and Characterization for CMOS Quanta Image Sensors. *Sensors*, *19*(24), 5459. https://doi.org/10.3390/s19245459

[18] Grüneis, F. (2019). An alternative form of Hooge's relation for 1/f noise in semiconductor materials. *Physics Letters A*, *383*(13), 1401–1409. https://doi.org/10.1016/j.physleta.2019.02.009

[19] Rehman, A., Smirnov, S., Krajewska, A., But, D. B., Liszewska, M., Bartosewicz, B., Pavlov, K., Cywinski, G., Lioubtchenko, D., Knap, W., & Rumyantsev, S. (2021). Effect of ultraviolet light on 1/f noise in carbon nanotube networks. *Materials Research Bulletin*, *134*, 111093. https://doi.org/10.1016/j.materresbull.2020.111093

[20] Kolodiy, Z. A. (2010). Flicker-noise of electronic equipment: Sources, ways of reduction and application. *Radioelectronics and Communications Systems*, *53*(8), 412–417. https://doi.org/10.3103/S0735272710080030

[21] Kolodiy, Z. A. & Mandziy, B. A. (2016). Calculation of Flicker Noise Power. *Automatic Control and Computer Sciences*, *50*(1), 15–19. https://doi.org/10.3103/S0146411616010041

[22] Ouyang, G., Hildebrandt, A., Schmitz, F., & Herrmann, C. S. (2020). Decomposing alpha and 1/f brain activities reveals their differential associations with cognitive processing speed. *NeuroImage*, *205*, 116304. https://doi.org/10.1016/j.neuroimage.2019.116304

[23] Dave, S., Brothers, T. A., & Swaab, T. Y. (2018). 1/f neural noise and electrophysiological indices of contextual prediction in aging. *Brain Research*, *1691*, 34–43. https://doi.org/10.1016/j.brainres.2018.04.007

Krzysztof Przystupa, Ph. D., works at the department of Automation, Faculty of Mechanical Engineering, Lublin University of Technology. Areas of scientific research: automation of technological processes, applied metrology, technological and functional quality and Internet of things.

Zenoviy Kolodiy, D.Sc., is Professor of the Department of Specialized Computer Systems of Lviv Polytechnic National University. His field of scientific interests are the study of electrical noise and the information essence of fluctuation processes. He is the author of more than 50 articles and 4 patents.

Jacek Majewski received his one M.Sc. degree in mechanical engineering in 1983 and another in electrical engineering and 1989. He also received his Ph.D. degree in electrical engineering in 1999 from the Lublin University of Technology. His field of scientific interest are sensors, digital measuring instruments and fundamentals of metrology.

Yuriy Khoma, Ph.D., D.Sc. is the author of more than 50 academic papers and articles. He is now Associate professor at Lviv Polytechnic National University. His research interests include machine learning, bioinformatics and large-scale analytics, natural language processing, computer vision, speech recognition and time series analysis.

Svyatoslav P. Yatsyshyn, D.Sc., is Professor of Information-Measuring Department of Lviv Polytechnic National University, Ukraine and Actual Member of International Thermoelectric Academy and of Ukrainian Academy of Metrology as well as Member of TC-12 IMEKO**.** He specializes in information-measuring temperature systems, nanometrology and nanothermometry, in materials science, methods and means of electrical and magnetic measurements, thermodynamics of non-equilibrium processes, and cyber-physical systems. He is the author of works on Quantum of Temperature and Quantum Temperature Standard, for example, those reported on 13^{th} International Symposium on Temperature and Thermal Measurements in Industry and Science under the auspices of TC12 IMEKO, Poland, Zakopane, 2016.

Iryna Petrovska, Ph. D., is Associate Professor at the Department of Measuring Information Technologies of the Institute of Computer Technologies, Automation and Metrology at Lviv Polytechnic National University. Her area of scientific research are resistive (conductive) tomographic systems, development as a mathematical apparatus for obtaining the most accurate, real-time reconstructed image of resistance or conductivity, and search for ways to achieve higher accuracy of image acquisition.

Serhiy Lasarenko is a Ph.D. student of metrology and information-measuring technology. He has performed research work in the field of methods and devices of measurements.

Taras Hut is a Ph.D. student of metrology and information-measuring technology. He has performed research work in the field of methods and devices of measurements.